

Study of Thickness Effect in Shear Layer Correction by CAA Simulation

Jin Jiao¹, Jan Delfs², Jürgen Dierke³

^{1,2,3} *Institut für Aerodynamik und Strömungstechnik*

Deutsches Zentrum für Luft- und Raumfahrt e.V.

Lilienthalplatz 7, 38108 Braunschweig, Deutschland

Email: Jin.Jiao@dlr.de, Jan.Delfs@dlr.de, Juergen.Dierke@dlr.de

Introduction

In the open jet wind tunnel experiments, the sound wave emitted from source must pass through a free shear layer induced by the open jet nozzle before reaching the microphones placed out of flow. The shear layer will alter both the amplitude and direction of sound waves, by means of refraction, reflection, scattering and spectral broadening effects. The refraction and reflection due to the velocity gradient is sketched in Fig. 1. When sound interacts with the shear layer, some parts of the energy travels through it but with an altered propagation direction (as drawn by red line), other parts are reflected back (as drawn in blue line). Currently the most widely used method is Amiet's approach to correct these two effects of the shear layer away from experimental data. However, the theory is derived by assuming a zero thickness shear layer, which may cause deviation from the real situation. So it is necessary to investigate how much effect the shear layer thickness bring into the data, to improve the experimental correction and data evaluation.

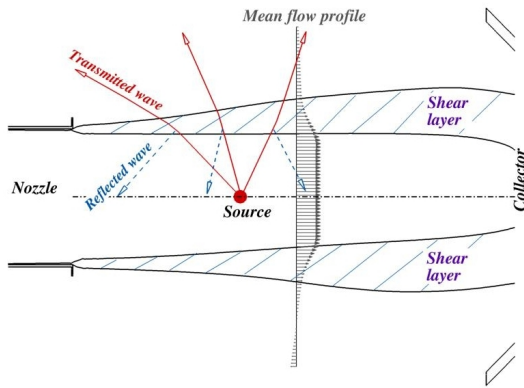


Figure 1: Sound transmission through the open jet shear layer in AWB.

This paper focuses on the refraction effects from planar shear layers while taking into account different thicknesses. The first study of thickness effects deals with a harmonic source at $1kHz$ and $10kHz$ in a shear flow with linear velocity profile, whose thickness varies from $0.1m$ to $0.5m$, $0.2m$ per step. This study is followed by 2D CAA simulations of the plane shear layer part of DLR's Acoustic Windtunnel Braunschweig (AWB) flow field. Finally, both angle and amplitude corrections in the theory are examined through comparisons with numerical results.

Amiet's theory

Based on geometrical acoustics and Ribner's solution for the transmission and reflection of sound by a plane zero-thickness shear layer [1], Amiet raised up a method for correcting acoustic wind tunnel measurements independent of source type [2]. The sketch in Figure 2 gives a straightforward view about the method, in which point M represents measurement position where the microphone is located in experiments, and point A is the corresponding corrected position where the sound wave would arrive in the absence of the shear layer. The amplitude measured at point M is firstly traced back to point C+ right above the shear layer, which is used to derive the value at point C- just below the shear layer through Ribner's solution. After that, the amplitude at point A could be got from the sound level at C- by the fact that sound pressure decays inversely as the distance from the source.

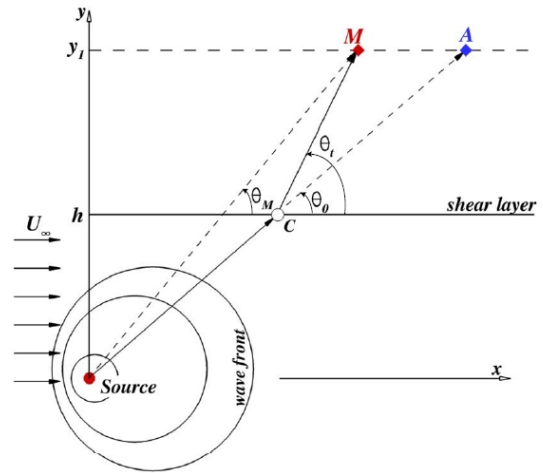


Figure 2: Amiet's method for zero thickness shear layer correction.

$$\tan \theta_0 = \frac{\zeta}{(1 - M^2) \cos \theta_t + M}$$

$$y_1 \cot \theta_M = h \cot \theta_0 + (y_1 - h) \cot \theta_t$$

$$\zeta = \sqrt{(1 - M \cos \theta_t)^2 - \cos^2 \theta_t} \quad (1)$$

$$\frac{\overline{p_A^2}}{\overline{p_M^2}} = \frac{h^2}{y_1^2} \frac{[\sin \theta_t + (y_1/h - 1)\zeta]}{\sin \theta_t} \frac{[\sin^3 \theta_t + (y_1/h - 1)\zeta^3]}{\sin^3 \theta_t}$$

$$\times \frac{[\zeta + \sin \theta_t (1 - M \cos \theta_t)^2]^2}{4\zeta^2} \quad (2)$$

Above are the equations derived in the approach, in which θ_M is the measurement angle, θ_0 represents the radiation angle and θ_t indicates the transmitted angle (also named as refracted angle). Based on the angle correction Eq. 1, the corrected position (A) could be determined for given measurement position (M). Afterwards the pressure amplitude at A will be calculated according to Eq. 2, of which the first term stands for amplitude change from point $C-$ to A , the second represents the intensity variation in the source-microphone plane, the third one gives the intensity variation in the normal-to-page direction, and the intensity jump through the shear layer. Additionally, special attention needs to be paid on two facts. One fact is that the intensity variation in the third dimension (second term) always equals to 1.0 in this paper since the simulation is two dimensional. Due to the same reason, for the transfer of the amplitude from $C-$ to A , the first term should be h/y_1 , since the ratio is proportional to root of the distance rather than distance itself.

Approach

Simulations are conducted for open jet flow field at 60m/s with CAA Code PIANO [3] developed at DLR. Firstly computations were operated for a harmonic source in constant thickness shear flows, of which the velocity profile in the shear layer part varies linearly in the vertical direction. The centerline was fixed at a distance 0.6m away from the source point ($h = 0.6\text{m}$), which coincides with the nozzle lip line position in AWB. Microphones were placed 1.2m from the source. Presented in Figure 3 are small sections of the three cases $\delta = 0.1\text{m}, 0.3\text{m}, 0.5\text{m}$, where δ represents the shear layer thickness. Arrowed lines give the velocity profile. The actual computation domain for each case covers an area of $10\text{m} \times 1.5\text{m}$ that aims at investigating the wave propagation characteristic in the far upstream and downstream directions. Simultaneously, sound propagation was simulated in a constant mean flow in which the velocity was kept constant (60m/s) for the entire domain to obtain the data at so-called 'corrected position A ' in the theory. Then the simulation is done in a 2D AWB flow, shown in Figure 4, which shows a plane shear layer with vertical velocity profiles similar to linear profiles. However, it can be seen that the shear layer spreads as the flow goes downstream, rather than staying constant as in the previous studies. This time-averaged mean flow field is obtained by DLR's inhouse CFD code TAU.

A harmonic source is applied and incoming waves are prescribed by a sponge layer boundary condition. The arc structure shown in Fig. 4 is generated to introduce the analytically known sound wave into the computational domain by the sponge layer.

Sound transmission through linear shear layer

To systematically study the characteristics of sound transmission through an analytical shear layer, linear ve-

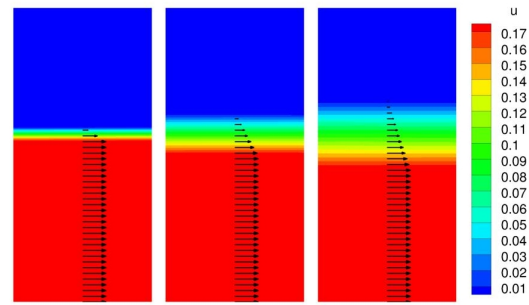


Figure 3: Shear flow with linear velocity profile (with arrowed lines give velocity profile). (From left to right: $\delta = 0.1\text{m}, 0.3\text{m}, 0.5\text{m}$)

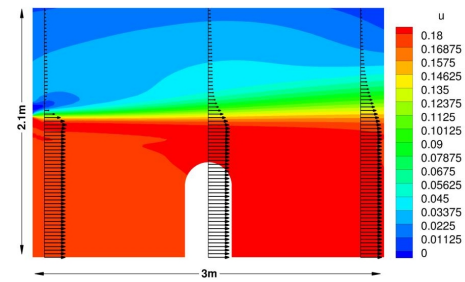


Figure 4: Plane shear layer in AWB.

locity profile shear flow is firstly applied in the simulations.

Fig. 5 illustrates the instantaneous pressure perturbation field at 1kHz and 10kHz in three thicknesses shear flow. The solid lines mark the upper and lower boundary of the shear layer, while the dash dot line gives the centerline of shear layer. Also plotted are the theoretical propagation paths derived from the angle correction Eq. 1 for three radiation angles, $\theta_0 = 45^\circ, 80^\circ, 135^\circ$. Corresponding transmission angles are given, too. We could see that the wave front obtained from CAA agrees well with theory even when the thickness significantly increases. Additionally, a strong total reflection was observed in the upstream direction, which becomes stronger as the thickness increased at both frequencies. The wave reflected from the shear layer interacts with the directly emitted sound wave to generate the interference pattern shown in the figure. Moreover, downstream a Mach wave is formed due to the sound wave acceleration by the mean flow below the shear layer. The Mach angle is 58° at mean flow velocity 60m/s . On the other side, the critical transmission angle θ_t^* defines the region into which any sound will not transmit through the shear layer since the wave hits the shear layer at an incidence angle equal to zero. That is the so-called zone of silence, which could not be seen in Fig. 5 since the incidence angle is always larger than zero due to size limitation of the computational domain.

To further examine about the thickness effect, Fig. 6 gives the sound pressure level (SPL) field for $\delta = 0.1\text{m}$ and 0.5m , in which the total reflection could be observed more apparently. Obviously, the reflection strength is stronger in the thicker case. At the same time, a low

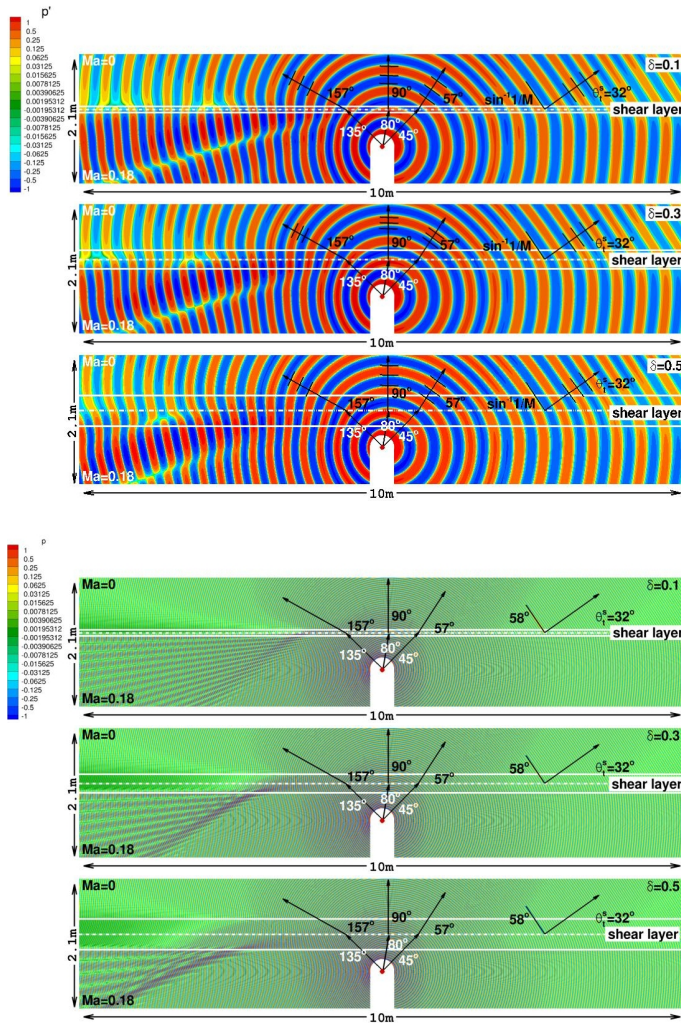


Figure 5: Sound propagation through linear shear layer at $1kHz$ and $10kHz$ at various thicknesses.

sound pressure level area is formed due to the interference between reflected wave and direct waves from source. There are still another two low noise areas around the shear layer upstream. In order to explain this phenomenon, a phase contour for $\delta = 0.1m$ around this region is given in Fig. 7, in which red circles indicate the region for low SPL. As shown in the figure, the transmitted wave propagates exactly against the flow direction beyond the point of total reflection in the shear layer. However, the adjacent sound wave traveling right below the shear layer does not experience such an effect. As a result, there is a phase shift in the interface, which is the reason for the low SPL distribution.

Sound transmission through 2D AWB shear layer

As shown in Fig. 1 and Fig. 4, the open jet shear layer expands upon going downstream. So the thickness varies at different sections in Fig. 4. Simulations are done in the flow field with same velocity $U_0 = 60m/s$. However, due to the size limitation of AWB test section, the CAA domain is reduced to $3m \times 1.5m$, which leads to a radiation angle range shrink.

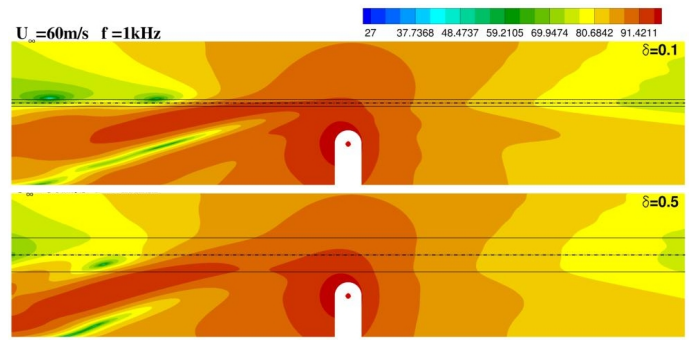


Figure 6: Sound pressure level field at $1kHz$.

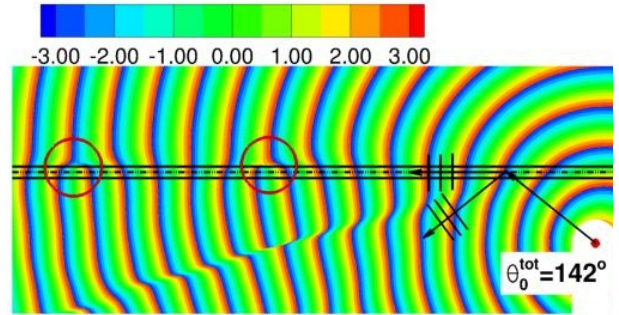


Figure 7: Simultaneous phase contour for $\delta = 0.1m$ at $1kHz$.

The pressure perturbation field is given in Fig. 8 at $1kHz$ (upper) and $10kHz$ (lower). Since the velocity below the shear layer is identical as for the linear case, the theoretical paths stay identical, still shown as black arrowed line. Centerline is defined as extending horizontally the nozzle lip position downstream, depicted as dash-dot line. The inner and out boundary of the shear layer are defined here like $U/U_0 = 0.95$ and $U/U_0 = 0.2$, plotted by white solid lines. The theoretical prediction matches still well CAA results. Moreover, the position of total reflection is quite close to the left boundary of the domain, which may be seen by the curved wave front around the region, but not as clear as in linear case.

Comparison with Amiet's method

Since the accuracy of the angle correction has been validated, this part will concentrate on confirmation of amplitude correction in Eq. 2. The procedure is carried out in several steps as below:

- The pressure amplitude p_M^2 is obtained on a line at a distance $y_1 = 1.2m$ away from the source through simulations of sound propagation in a shear flow (as shown in Fig. 3 and 4).
- Based on Eq. 1, the corresponding corrected position A could be fixed for each point M on the line in the first step.
- The pressure amplitude p_A^2 is generated by simulating the propagation in a constant mean flow field without shear layer.
- Comparison between theoretical value got from Eq.

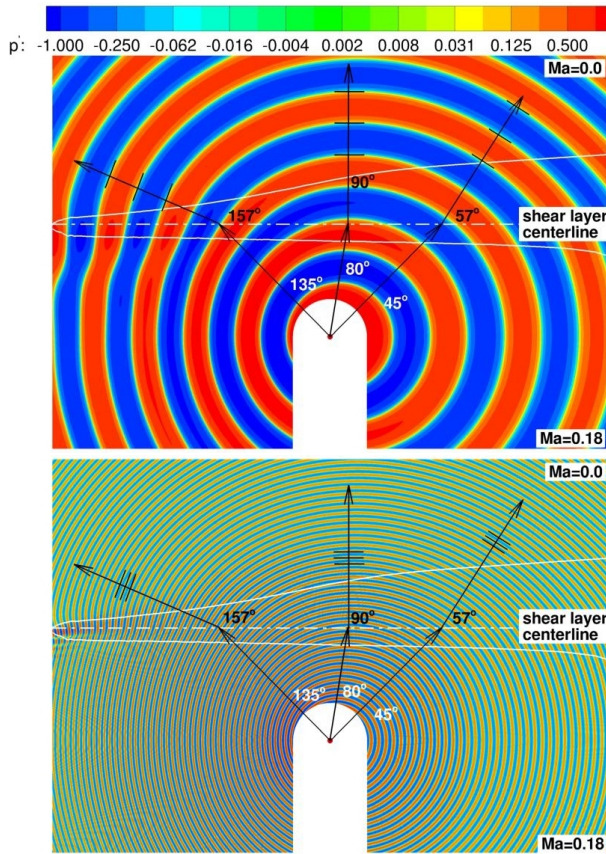


Figure 8: Sound transmission through 2D AWB shear layer.

2 and ratio of pressure gained from step *a* and *c*.

Concerning the measurement in AWB flow field a narrower angle area is covered than in the linear case, the horizontal axis in Fig.9 gives the angle range for AWB flow field domain. Since θ_M is measured relative to flow direction, values larger than 90° represent upstream propagation conversely. Solid lines represent the correction curves at 1kHz , while points for 10kHz . Evidently, the smallest deviation between CAA and the theory is for $\delta = 0.1m$. The deviation goes up as the thickness increases. The curve for the AWB shear layer got the largest difference, which may be caused by the spreading shape and non-linear velocity profile of the shear layer. Another phenomenon to be noticed is that the curve is not significantly affected by the source frequency. It is seen that an amplitude correction is not necessary anymore at angles around 85° since the sound wave travels through the shear layer at incident angle 90° without any refraction.

Conclusion

Systematical numerical simulations were carried out for the sound transmission through plane 2D shear layers for two types of shear flow at high and low frequencies. By observing the radiation characteristic around total reflection, it is found that several low sound pressure level area was formed and the thickness can alter the position and strength of reflected wave. The total reflection point is pushed more upstream as the thickness increases. The

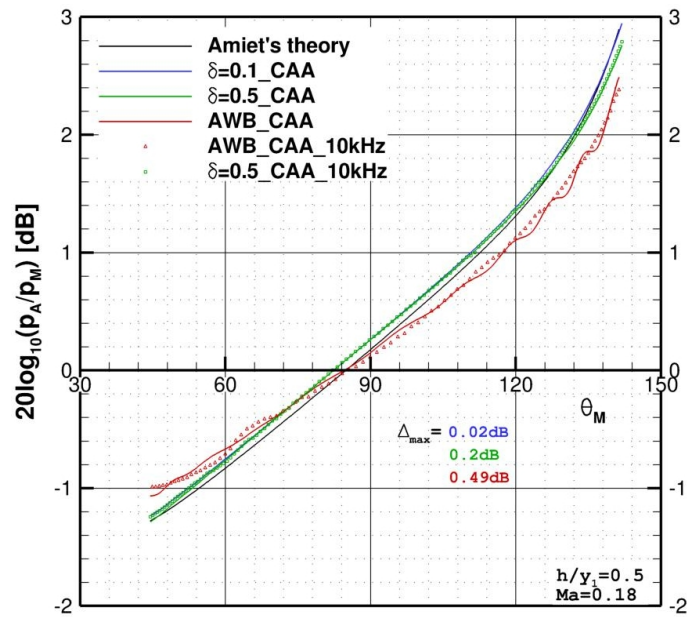


Figure 9: Comparisons of amplitude correction.

deviation between CAA results and theoretical values in comparison of amplitude correction goes up as the thickness increases. The maximum difference is 0.49dB, which appears in AWB flow field. The reason for this might be the spreading shape and non-linear velocity profile of the shear layer. By comparison, one also observes that the correction curve was not affected significantly by the frequency.

References

- [1] Ribner, H. S.: Reflection, transmission and amplification of sound by a moving medium, Journal of the Acoustical Society of America, Vol. 29, 1957, 435-441
- [2] Amiet, R. K.: Correction of open jet wind tunnel measurements for shear layer refraction, AIAA Conference on the Exploration of the Outer Planets, Vol. 1, 1975
- [3] Delfs, J., Bauer, M., Ewert, R., Grogger, H., Lummer, M., and Lauke, T.: Numerical simulation of aerodynamic noise with DLR's aeroacoustics code PIANO, Tech. rep., DLR, PIANO manual for version 5.2, 2008